SURFICIAL GEOLOGY OF THE CHICXULUB IMPACT CRATER, YUCATAN, MEXICO

KEVIN O. POPE,[1] ADRIANA C. OCAMPO,[2] and CHARLES E. DULLER[3]

[1]*Geo Eco Arc Research, 2222 Foothill Blvd. Suite E-272, La Canada, CA 91011, U.S.A.*
[2]*MS 183–601, Jet Propulsion Laboratory, 4800 Oak Grove Dr., Pasadena, CA 91109, U.S.A.*
[3]*MS 242–4, NASA Ames Research Center, Moffett Field, CA 94035, U.S.A.*

Abstract. The Chicxulub impact crater in northwestern Yucatan, Mexico is the primary candidate for the proposed impact that caused mass extinctions at the end of the Cretaceous Period. The crater is buried by up to a kilometer of Tertiary sediment and the most prominent surface expression is a ring of sink holes, known locally as cenotes, mapped with Landsat imagery. This 165 ± 5 km diameter Cenote Ring demarcates a boundary between unfractured limestones inside the ring, and fractured limestones outside. The boundary forms a barrier to lateral ground water migration, resulting in increased flows, dissolution, and collapse thus forming the cenotes. The subsurface geology indicates that the fracturing that created the Cenote Ring is related to slumping in the rim of the buried crater, differential thicknesses in the rocks overlying the crater, or solution collapse within porous impact deposits. The Cenote Ring provides the most accurate position of the Chicxulub crater's center, and the associated faults, fractures, and stratigraphy indicate that the crater may be ~240 km in diameter.

Introduction

The Chicxulub structure in northern Yucatan, Mexico was first interpreted as an impact crater based upon the discovery of a concentric pattern of magnetic and gravimetric anomalies (Penfield and Camargo, 1981). A series of recent findings indicate that the Chicxulub structure is the long sought after impact crater whose iridium-rich ejecta blanketed much of the globe at the Cretaceous/Tertiary (K/T) boundary, and which probably caused the mass extinctions that mark this geologic transition (Alvarez *et al.*, 1980). Briefly listed, these findings come from studies of: (1) mineral grains with shock metamorphism at Chicxulub (Hildebrand *et al.*, 1991; Sharpton *et al.*, 1992); (2) circular hydrogeologic anomalies that correlate with the magnetic and gravimetric anomalies (Pope *et al.*, 1991); (3) the unique chemistry of the Chicxulub impact melt rock and its similarity to glassy K/T ejecta in Haiti and target rock at Chicxulub (Sigurdsson *et al.*, 1991; Kring and Boynton, 1992); (4) K/T impact ejecta thicknesses relative to the size and location of Chicxulub (Hildebrand and Boynton, 1990; Hildebrand, 1992; Vickery *et al.*, 1992); (5) impact-generated tsunami wave deposits in the Gulf of Mexico (Hildebrand and Boynton, 1990; Smit *et al.*, 1992; Alvarez *et al.*, 1992); and (6) the radiometric age (65.0 million years ago) of the Chicxulub impact melt and Haiti K/T tektites (Swisher *et al.*, 1992).

In this paper we expand upon our earlier work (Pope *et al.*, 1991) and examine

Earth, Moon, and Planets **63**: 93–104, 1993.

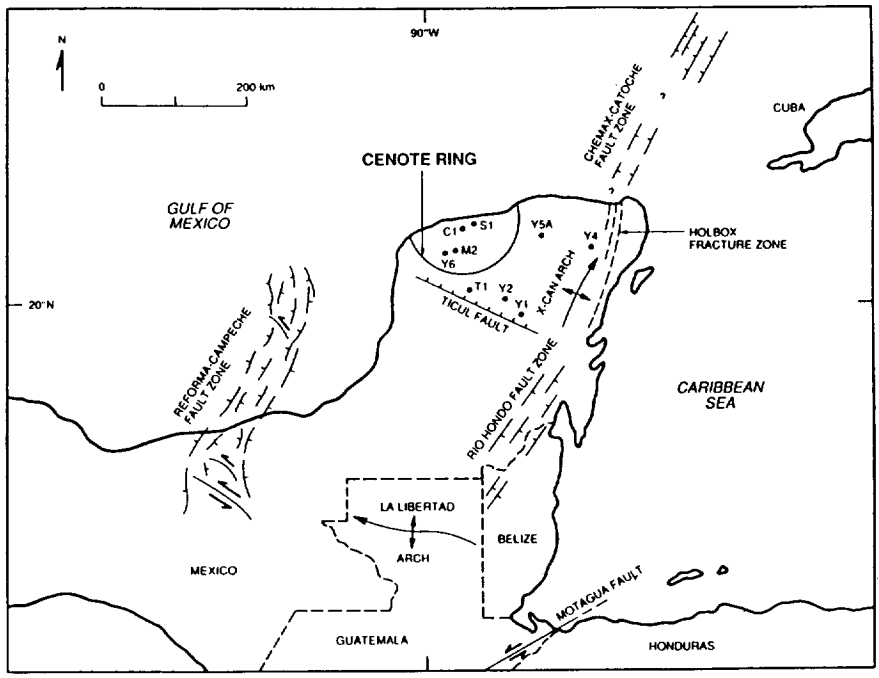

Fig. 1. Tectonic features of the Yucatan Peninsula (modified from Weidie, 1985 and interpretation of TM imagery). Note locations of exploratory wells (well names given in Figure 6).

in detail the surface evidence for the buried Chicxulub crater. We combine analyses of satellite and geological data to elucidate the unique geology of northern Yucatan, which we propose developed as a result of an asteroid or comet impact 65 million years ago.

Geomorphology

The northern coastal plain of the Yucatan Peninsula is bounded by the Ticul Fault, Gulf of Mexico, and Caribbean Sea (Figure 1). The plain is a region of youthful karst development (Isphording, 1975, 1977), and is composed primarily of uplifted sections of Early and Late Tertiary platform carbonates, with a band of Quaternary beach and lagoon deposits along the coast (Figure 2). There are two main fracture systems within the plain: the Holbox Fracture Zone in the east (Weidie, 1982, 1985), and a system in the west whose salient feature is a semi-circular boundary between zones of fractured and unfractured rock (Pope *et al.*, 1991) (Figures 1 and 2). The fracture patterns are interpreted primarily from solution features in the Tertiary limestones (Anonymous, 1983). A chain of sink holes is found along this boundary zone, named the Cenote Ring (cenote is the local name for sink

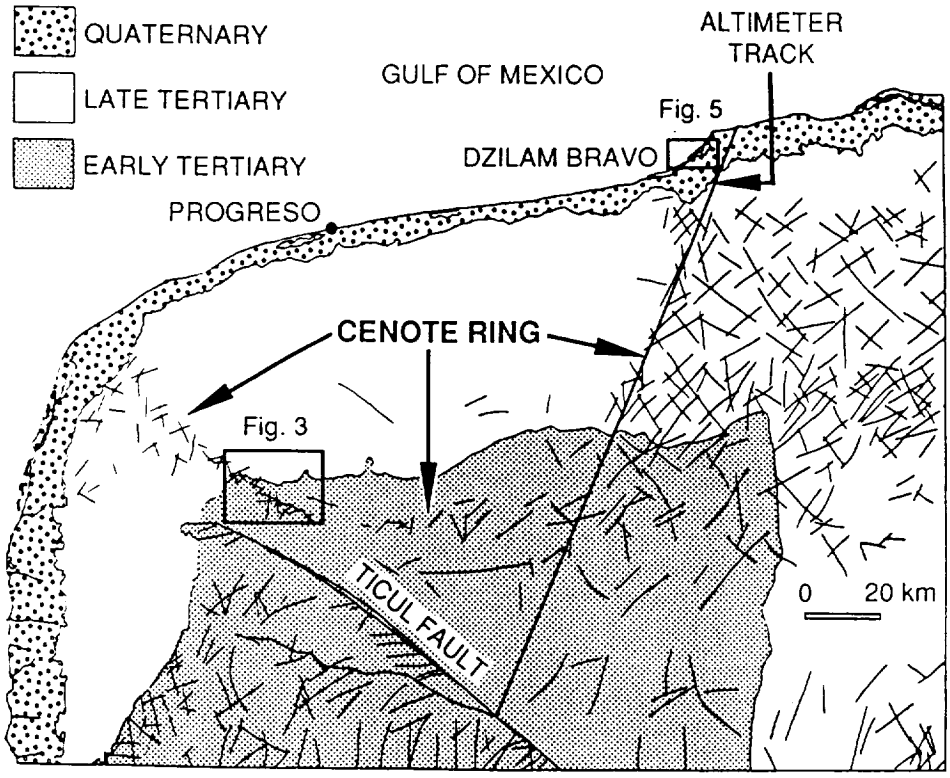

Fig. 2. Geological map of northwestern Yucatan (Anonymous 1983) showing relationship between Cenote Ring and regional fracture patterns. Compiled from sheets F16-7, F15-9-12, and F16-10.

hole, adapted from the Yucatec Maya word *dz'onot* (Hall, 1936)). The Cenote Ring was first described using Landsat Thematic Mapper (TM) imagery during a survey of water resources (Pope and Duller, 1989).

The Cenote Ring contains over two hundred cenotes, which range in size from 50 to 500 m wide and 2 to over 120 m deep (Hall, 1936; Soki *et al.*, 1984). The ring is a nearly perfect 165 ± 5 km diameter semi-circle, truncated by the coast, and centered on the coast 17 km east of Progreso (Figure 2). Cenote density along the ring varies from 3 cenotes/km^2 in a 3 km wide band of cenotes in the southwest (Figure 3), to a chain of single cenotes 3 km apart in the southeast. The northeastern portion of the Cenote Ring is best described as a boundary between a zone of abundant cenotes to the east and few to no cenotes to the west (inside) of the ring. Southwest of the Cenote Ring is a possible second partial ring. It is composed of over 10 cenotes in a concentric arc with a radius of 92 km from the Cenote Ring center.

A topographic profile across the region from the Seasat radar altimeter (Figure

Fig. 3. Landsat TM band 5 (in red), 4 (in green), and 3 (in blue) image (April, 1985) of the southwestern portion of the Cenote Ring (location shown in Figure 1). Note chain of black (and occasionally blue-green) dots across center of image. These dots are cenotes: collapsed solution cavities that intersect the water table. Image width is 15 km. Landsat data from EOSAT Co., Lanham, MD.

4) shows that the three geologic units of the plain form distinct geomorphic surfaces. The early Tertiary carbonate surface has a different slope and is much more dissected (karstified) than the late Tertiary one. The profile also shows that while on the macroscale the late Tertiary surface is the smoothest, it contains a series of depressions 5–10 m deep where the profile crosses the Cenote Ring. (Figure 4). These depressions contain the cenotes and have a common base level, which approximates the regional water table (Marin, 1990).

Hydrology

The hydrology of the plain is largely controlled by fractures in the flat Tertiary limestones (e.g., Back *et al.*, 1979; Hanshaw and Back, 1980; Back *et al.*, 1986; Marin, 1990). The aquifer in northwestern Yucatan is unconfined, except near the coast where an impermeable caliche has formed near the surface along the zone of fresh water discharge as it migrated inland with rising Holocene sea level (Perry *et al.*, 1989). This aquitard varies in width from 5 km near the northeastern terminus of the Cenote Ring to 30 km near the southwestern end of the ring. As indicated by the fracture pattern noted above, solution features inside the ring are rare, but are abundant along and outside of the ring. Except for the partial second ring noted above, there are few solution features southwest of the ring. This is due possibly to the presence of the impermeable caliche layer, which has sealed surface cracks. This paucity of detected fractures may also reflect the fact that both rainfall (ca. 500 mm/yr) and elevation (less than 8 m above mean sea level)

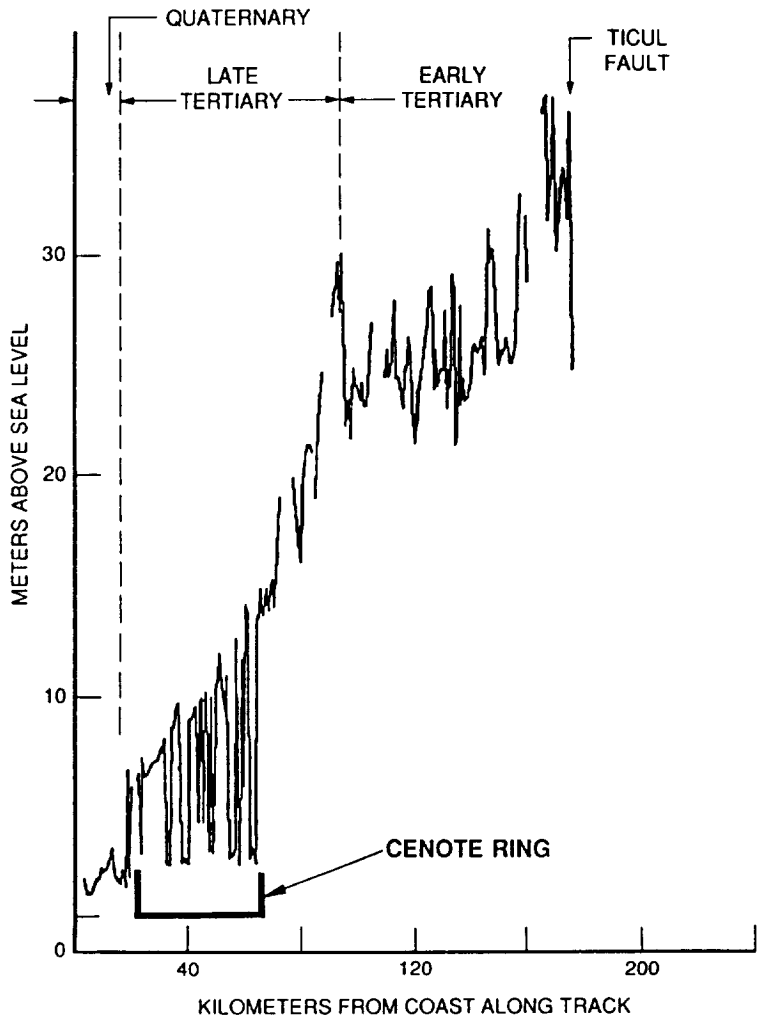

Fig. 4. Topographic profile (location shown in Figure 2) from Seasat radar altimeter. The coastal plain is composed of three geomorphic surfaces: a coastal zone with Quaternary beach and lagoon sediments, a smooth Late Tertiary surface, and a rough, karstified Early Tertiary surface. The altimeter lost lock on the ground surface at the 100 m high escarpment of the Ticul Fault, which demarcates the southern boundary of the coastal plain. The altimeter profile falls within the Cenote Ring between 20 and 70 km inland along track. Seasat altimeter profile is from track No. 43744. Heights are with respect to the geoid, therefore elevations above mean sea level are approximate. Seasat data provided by H. Frey, NASA Goddard Space Flight Center.

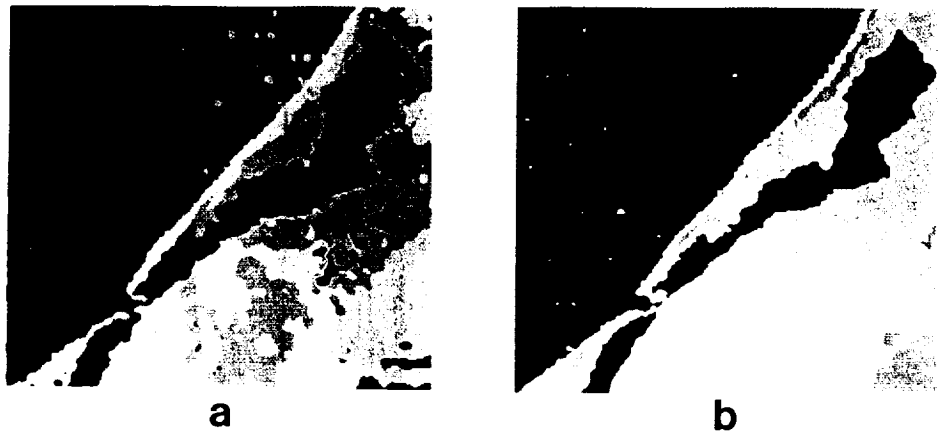

Fig. 5. Landsat TM band 6 (thermal infrared) images near Dzilam Bravo, northeastern terminus of Cenote Ring (north at top, location shown in Figure 1): (a) wet season, October 1986, (b) dry season, April, 1985. Sea-surface cold water anomalies are color-coded black. Light blue areas are warm sea water and dark blue areas slightly cooler. Warm land surfaces are in cream, yellow, and red. The gray and light blue areas inland from the northern lagoon in the wet season image are clouds and cloud shadows. The black anomalies, interpreted as fresh water spring discharge from the Cenote Ring, appear within the coastal lagoon and along the seaward side of the beach ridge in the lower left-hand (southwest) portion of the wet season (a) image. Spring discharge appears to be greatly reduced in the dry season image. The black area offshore is cold, deep, marine water. The TM sensor recorded a sea-surface temperature of ~26 °C (light blue), and cold water anomalies (springs) of ~23 °C (black). These temperatures are uncorrected for atmospheric effects, and are computed using equations from Marlaret *et al.* (1985). Sea-surface and spring temperatures of 30 °C and 27 °C respectively are reported from *in situ* measurements in the southeastern Yucatan Peninsula (Back *et al.*, 1979). Differences in the absolute temperatures are due to cooling effects of the atmosphere in the satellite measurements, however the temperature gradients are similar. Image width is 9 km. Landsat data from EOSAT Co., Lanham, MD.

are the lowest in this region and solution features are greatly subdued. Ground water flows toward the coast along these fractures until reaching the ring, which acts as a barrier that intercepts the flow. The resulting increased subsurface flow along the ring has created a system of caves and conduits whose collapse formed the cenotes.

Ground water flow along the ring is indicated by a valley-shaped depression in the ground water surface centered on the ring (Marin, 1990). Additional evidence is found along the coast where large fresh water springs occur. Landsat TM thermal infrared (band 6) imagery of the northeast terminus of the Cenote Ring near Dzilam Bravo contains several cold thermal anomalies along the barrier beach and in the brackish lagoon (Figure 5). We interpret these anomalies as discharges of cold, fresh water from springs reported from this area (Isphording, 1977). Cold water anomalies are very rare along the coast within the Cenote Ring and east of the ring terminus. Where they do occur, they are smaller than those near Dzilam

Bravo. A major exception occurs at the terminus of the Holbox fracture zone where huge cold water anomalies are found, which indicate a high discharge of fresh water (Duller and Pope in press). Wet and dry season TM imagery of the northeastern ring terminus reveals that spring discharge responds to seasonal rains (Figure 5), consistent with water table fluctuations (Marin, 1990). We have not analyzed TM imagery of the western ring terminus, but we observed many springs there during a 1993 reconnaissance trip.

Subsurface Geology

We examined data from nine exploratory oil wells drilled by Petroleos Mexicanos (PEMEX) in the vicinity of the Cenote Ring (Figure 1). The well data show that the ring interior corresponds with a Late Cretaceous structural low filled with undeformed Tertiary sediments (Figure 6). We lack well data from north of the ring, although seismic data there do indicate a drop in the K/T surface within the suspect crater rim (Hildebrand *et al.*, 1991). Beneath the Tertiary carbonates that fill the basin are a series of impact breccias and melt, overlain by probable slump deposits. The upper-most Cretaceous strata outside the basin are conglomerates and breccias (Weidie, 1985). Underlying this unit is a 2.5 km thick sequence of Cretaceous carbonates and evaporites underlain by a thin sequence of Jurrasic sediments resting on a Paleozoic metamorphic basement. When the well data are plotted as a function of their radial distance from the crater center, offsets in the Cretaceous and earlier rocks beneath the conglomerate/breccia unit are apparent. These offsets are interpreted as possible normal faults, and one such fault is recorded in well T1.

Discussion

Previously, we hypothesized that the Cenote Ring and its associated fracture system are the result of post-impact subsidence in the rim of the Chicxulub crater (Pope *et al.*, 1991). The zone of fracturing outside of the ring corresponds with our zone of inferred normal faulting, and subsidence along these faults is a possible cause of the fractures. These faults may be ring faults with their associated terrace zone containing slump blocks. If the Cenote Ring (~170 km dia.) corresponds with the crater floor, then a rim diameter of 240 km and a 35–40 km wide terrace zone of slump blocks are predicted using the morphometric relationships established for extraterrestrial impacts (Melosh, 1989). These dimensions are consistent with our inferred zone of faulting outside the Cenote Ring.

The inferred fault between the Y1 and Y4 wells, as well as the surface fracturing in the same area, are outside our postulated zone of ring faulting. These outer features may not be related to the impact structure. Nevertheless, impact craters of this magnitude are usually complex structures with multiple concentric features (e.g., Croft, 1985; Pike, 1985). Therefore ring faults like those discussed above

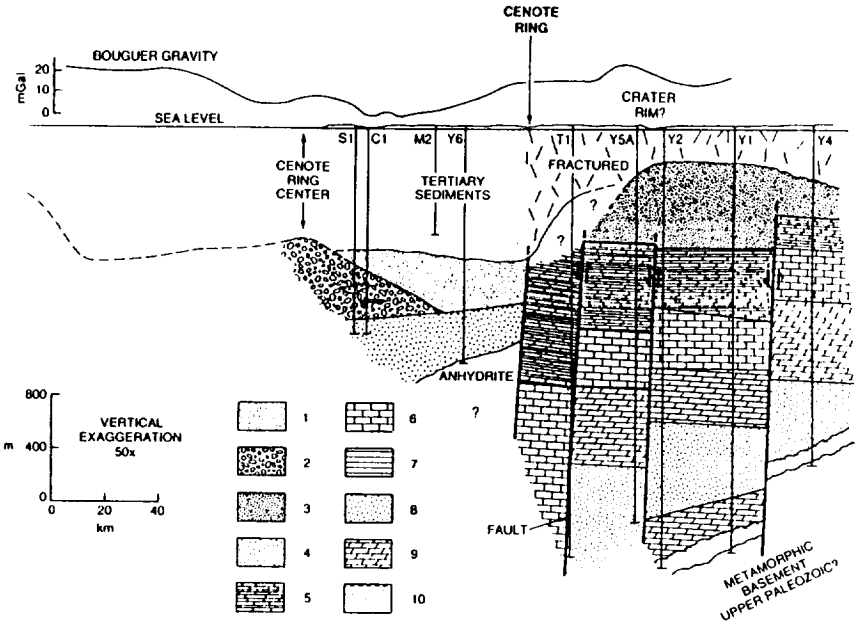

Fig. 6. Subsurface geology of the Cenote Ring based on well data (well locations in Figure 1). Wells are plotted as a function of their radial distance from the center of the Cenote Ring. Stratigraphy and description of lithofacies of Yucatan 1 (Y1), Yucatan 2 (Y2), Yucatan 4 (Y4), Yucatan 5A (Y5A), and Yucatan 6 (Y6) are from Marshall, 1974 as modified in Weidie, 1985. Lithofacies and correlations from Sacapuc 1 (S1), Chicxulub 1 (C1), and Ticul 1 (T1) are our own, based on stratigraphic profiles presented by Lopez Ramos, 1979, and an unpublished version by G. E. Murray, A. A. Meyerhoff, and A. E. Weidie provided to us by A. E. Weidie. Thickness of Tertiary section and information on Merida 2 (M2) from Lopez Ramos, 1979). All faults except the one recorded in the Ticul 1 well are inferred from offset of beds. Gravimetric profile is from data in Hildebrand *et al.*, 1991 and is drawn through the Cenote Ring center and well Y4. Units 1, 2, 3, and 4 were originally designated as Upper Cretaceous (Lopez Ramos, 1979; Weidie, 1985), however the radiometric age of 65.0 million years (Swisher *et al.*, 1992) for the unit 4 melt rock indicates that units 1 and 2 are K/T boundary or later units. Unit 3 contains Upper Cretaceous fossils, but we suggest that this unit is also of impact origin and is a K/T boundary unit as well (see text). Key (interpretations in parentheses): 1 – Marl, sandstone, shale, and bentonite; the uppermost sediments in Yucatan 6 are globigerinid biomicrites (post-impact slump and backwash crater fill deposits). 2 – Bentonitic breccia (impact breccia). 3 – Conglomerate and breccia composed of angular to rounded pebble-sized detrital clasts of anhydrite, dolomite, and limestone in a dolomitic micrite matrix (reworked continuous deposit from secondary impacts). 4 – Andesite, andesitic tuffs, and glass (impact melt and suevite). 5 – Upper Cretaceous mollusc, pelletoid micrite and laminated fossiliferous dolomite. The Upper Cretaceous section in the Ticul 1 well contains abundant marls and the upper portion may correlate with unit 1 rather than 5. 6 – Lower Cretaceous pelleted rudist biomicrite, biosparite, and milinolid pelmicrite. 7 – Lower Cretaceous laminated dolomite. 8 - Lower Cretaceous anhydrite. 9 – Lower Cretaceous milinolid dolomite and quartz-silty dolomite. 10 – Jurassic (?) arenite, shale, anhydrite, and dolomite.

are expected and concentric tectonic features at large diameters are also possible. The curvature of the Holbox fracture zone (Figure 1) may be partly controlled by buried impact structures.

Given the age of the fractured rocks, the proposed subsidence would have occurred in or after the late Tertiary – many millions of years after the impact. Long-term tectonic instability of extraterrestrial impact craters has been proposed (e.g., Thomas *et al.*, 1982; Moore and Ahern, 1983), but remains speculative. Seismic studies of terrestrial craters indicate that no significant tectonic movement occurs after a few million years (Solomon and Duxbury, 1987). These terrestrial studies were limited mostly to craters that were much smaller and older than Chicxulub, and often deeply eroded, thus the relevance to Chicxulub is uncertain. Theoretical models predict that the rim height would reach equilibrium with gravity soon after impact (Melosh, 1989). Such models do not preclude subsidence in the rim due to burial by Tertiary sediments, or movement along ring faults in response to other tectonic forces.

Although the northern Yucatan Peninsula is not a tectonically active region today, the emergence of the northern peninsula and the formation of the Ticul fault in the Tertiary indicate that tectonism has occurred during the proposed period of crater rim subsidence. Given these regional stresses another mechanism that may account for the fracture pattern is differential fracturing due to the thickness of the Tertiary rocks. The Tertiary strata overlying the crater floor are 3 times thicker than the strata outside the rim, therefore these thinner strata are much more susceptible to fracturing. The abrupt change in thickness near the Cenote Ring may actually concentrate stresses there.

A non-tectonic hypothesis for the formation of the Cenote Ring was proposed by Perry *et al.* (1992), who suggested that a coral reef may have formed in the shallow water of the crater rim, and that solution collapse within the more porous reef facies has propagated upward to the surface. If this hypothesis is correct, then these early Tertiary reefs must have been much more extensive than Perry *et al.* suggest, because the solution features are not limited to the vicinity of the Cenote Ring. The suggestion that the surface solution features are related to the upward propagation of deep-seated solution collapse features may, however, be a plausible mechanism. Such deep solution collapse could have originated within the highly porous conglomerate/breccia unit. We propose that this unit is the product of secondary cratering by ejecta, following the process described by Overbeck (1975). The final distribution and conglomeritic texture of this unit probably resulted from the reworking processes described for marine impacts (Overbeck *et al.*, 1993). The conglomerate/breccia unit is extensive (Figure 6), and its distribution roughly corresponds with the surface fracture pattern that created the Cenote Ring.

Our suggested rim diameter of ~240 km is greater than the 180 km proposed by Hildebrand *et al.* (1991), which was based on airborne geophysical data. Information from the Ticul 1 well is critical to the placement of the crater rim; our assessment places this well within the crater and Hildebrand and colleagues place

it outside. Both the basin morphology and the Late Cretaceous lithologies support the placement of the Ticul 1 section within the crater.

The well data (Figure 6) show that the highest point of the basin rim is close to our crater rim estimate of ~240 km, and that the K/T boundary in the Ticul 1 well is depressed about 230 m below this proposed rim. The brief descriptions of the Upper Cretaceous strata in Ticul 1 indicate that these strata are unlike Upper Cretaceous strata outside the rim (Lopez Ramos, 1979), and apparently the conglomerate/breccia unit in Yucatan 5A does not extend as far as the Ticul 1 well (unfortunately no detailed description of the Ticul 1 well has been published). The Upper Cretaceous strata in Ticul 1 include abundant marls, which are not present in adjacent wells outside the crater, but are present in the deposits interpreted as post-impact slump overlying the impact melt (in the Y6, C1, and S1 wells). We suggest that the upper portion of the Cretaceous section in Ticul 1 may also be post-impact slump deposits. It should be noted that the slump deposits inside the crater were originally assigned to the Upper Cretaceous (Lopez Ramos, 1979), but radiometric dating of the underlying impact melt (Swisher *et al.*, 1992) combined with a re-appraisal of the paleontology (Hildebrand *et al.*, 1991) confirms that these sediments are K/T boundary or later deposits.

Conclusion

A large body of evidence now exits indicating that a large comet or asteroid impact occurred at Chicxulub at the end of the Cretaceous Period. The Cenote Ring and its hydrogeological properties add to the unique character of this event in geological history. The hydrogeological data help confirm the circular form of the Chicxulub structure, and given the nearly perfect circularity of the Cenote Ring and its inferred relationship to the buried crater, the ring's center provides a more accurate location for the crater's center than do the geophysical data.

We identified several possible mechanisms related to the impact that may have formed the Cenote Ring. The actual process may well be a combination of these mechanisms. Many uncertainties remain about the crater, the most relevant to this study are its size and details of its structure. The hydrogeological data shed light on these issues and indicate that Chicxulub may be ~240 km in diameter, which is much larger than previous estimates. Nevertheless, the exact size remains uncertain and future research on this well preserved and perhaps largest known terrestrial impact crater is needed.

Acknowledgements

Support for this research was provided by the NASA Exobiology Program to Geo Eco Arc Research and the Jet Propulsion Laboratory, and by the Directors Discretionary Fund to NASA Ames Research Center. We thank Alfred Weidie for providing unpublished stratigraphic profiles of the Yucatan Peninsula.

References

Alvarez, L. W., Alvarez, W., Asaro, F., and Michel, H. V.: 1980, 'Extraterrestrial Cause for the Cretaceous-Tertiary Extinction', *Science* **208**, 1095–1108.

Alvarez, W., Smit, J., Lowrie, W., Asaro, F., Margolis, S. V., Claeys, P., Kastner, M., and Hildebrand, A. R.: 1992, 'Proximal Impact Deposits at the Cretaceous-Tertiary Boundary in the Gulf of Mexico: A Restudy of DSDP Leg 77 Sites 536 and 540', *Geology* **20**, 697–700.

Back, W., Hanshaw, B. B., Pyle, T. E., Plummer, L. N., and Weidie, A. E.: 1979, 'Geological Significance of Groundwater Discharge and Carbonate Dissolution to the Formation of Caleta Xel Ha, Quintana Roo, Mexico', *Water Resources Research* **15**, 1521–1535.

Back, W., Hanshaw, B. B., Herman, J. S., and Van Driel, J. N.: 1986, 'Differential Dissolution of a Pleistocene Reef in the Groundwater Mixing Zone of Coastal Yucatan, Mexico', *Geology* **14**, 137–140.

Carta Geologica: 1983, 1:250,000: Mexico, Secretaria de Programacion y Presupuesto.

Croft, S. K.: 1985, 'The Scaling of Complex Craters', *Proceedings of the 15th Lunar and Planetary Science Conference, Part 2, Journal of Geophysical Research* **90**, C828–C842.

Duller, C. E. and Pope, K. O.: in press, *The Yucatan Peninsula, Land of the Maya: Views from Space*, Mexico, Council Nacional de Ciencias y Tecnologia.

Hall, F. G.: 1936, 'Physical and Chemical Survey of Cenotes of Yucatan', in *The Cenotes of Yucatan: Carnegie Institute of Washington Publication* **457**, 5–16.

Hanshaw, B. B. and Back, W.: 1980, 'Chemical Mass-Wasting of the Northern Yucatan Peninsula by Groundwater Dissolution', *Geology* **8**, 222–224.

Hildebrand, A. R.: 1992, 'K/T Boundary Ejecta Distribution Predicts Size and Location of Chicxulub Crater', *Lunar and Planetary Science* **XXIII**, 537–538.

Hildebrand, A. R. and Boynton, W. V.: 1990, 'Proximal Cretaceous-Tertiary Boundary Impact Deposits in the Caribbean', *Science* **248**, 843–847.

Hildebrand, A. R., Penfield, G. T., Kring, D. A., Pilkington, M., Camargo, A., Jacobsen, S. B., and Boynton, W. V.: 1991, 'Chicxulub Crater: A Possible Cretaceous/Tertiary Boundary Impact Crater on the Yucatan Peninsula, Mexico', *Geology* **19**, 867–871.

Isphording, W. C.: 1975, 'The Physical Geology of Yucatan', *Transactions of the Gulf Coast Association of Geological Societies* **25**, 231–262.

Isphording, W. C.: 1977, 'Geomorphic Evolution of Tropical Karst Terrains', in Tolson, J. S. and Doyle, F. L. (eds.), *Karst Hydrogeology*, Huntsville, University of Alabama Press, pp. 115–129.

Kring, D. A. and Boynton, W. V.: 1992, 'Petrogenesis of an Augite-Bearing Melt Rock in the Chicxulub Structure and its Relationship to K/T Impact Spherules in Haiti', *Nature* **358**, 141–144.

Lopez Ramos, E.: 1979, *Geologia de Mexico*, Tomo 3: Mexico, 445 pp.

Marin, L. E.: 1990, *Field Investigations and Numerical Simulation of Ground-water Flow in the Karstic Aquifer of Northwestern Yucatan, Mexico*, Ph.D. Thesis: DeKalb, University of Northern Illinois, 183 pp.

Marshall, R. H.: 1974, *Petrology of Subsurface Mesozoic Rocks of the Yucatan Platform, Mexico*, Masters Thesis: New Orleans, University of New Orleans, 97 pp.

Marlaret, E., Bartolucci, L. A., Lozano, D. F., Anuta, P. E., and McGillen, C. D.: 1985, 'Landsat-4 and Landsat-5 Thematic Mapper Data Quality Analysis', *IEEE Transactions on Geoscience and Remote Sensing* **20**, 1407–1416.

Melosh, H. J.: 1989, *Impact Cratering: A Geologic Process*, Oxford University Press, New York, 245 pp.

Moore, J. M. and Ahern, J. L.: 1983, 'The Geology of Tethys', *Proceedings of the 13th Lunar and Planetary Science Conference, Journal of Geophysical Research* **88**, A577-A584.

Overbeck, V. R.: 1975, 'The Role of Ballistic Erosion and Sedimentation in Lunar Stratigraphy', *Review of Geophysics and Space Physics* **13**, 337–362.

Overbeck, V. R., Marshall, J. R., and Aggarwal, H.: 1993, 'Impacts, Tillites, and the Breakup of Gondwanaland', *Journal of Geology* **101**, 1–19.

Perry, E., Swift, J., Gamboa, J., Reeve, A., Sanborn, R., Marin, L., and Villasuso, M.: 1989, 'Geologic and Environmental Aspects of Surface Cementation, North Coast, Yucatan, Mexico', *Geology* **17**, 818–821.

Perry, E. C., Winter, D. J., Sagar, B., and Wu, B.: 1992, 'The Chicxulub Structure: Surface Manifestation and Possible Sulfur Isotope Signature', *Lunar and Planetary Science* **XXIII**, 1057–1058.

Penfield, G. T. and Camargo, A.: 1981, 'Definition of a Major Igneous Zone in the Central Yucatan Platform with Aeromagnetics and Gravity', *51st Annual Meeting of the Society of Exploration Geophysicists*, Abstracts, p. 37.

Pike, R. J.: 1985, 'Some Morphologic Systematics of Complex Impact Structures', *Meteoritics* **20**, 49–68.

Pope, K. O. and Duller, C. E.: 1989, 'Satellite Observations of Ancient and Modern Water Resources in the Yucatan Peninsula', in R. Alvarez (ed.), *Simposio Latinamericano Sobre Sensores Remotos, Memoria*, Mexico, Sociedad de Especialistas Latinamericano en Percepcion Remota and Instituto de Geografia, Universidad Nacional Autonoma de Mexico, pp. 91–98.

Pope, K. O., Ocampo, A. C., and Duller, C. E.: 1991, 'Mexican Site for K/T Impact Crater?', *Nature* **351**, 105.

Sharpton, V. L., Dalrymple, G. B., Marin, L. E., Ryder, G., Schuraytz, B. C., and Urrutia-Fucugauchi, J.: 1992, 'New Links Between the Chicxulub Impact Structure and the Cretaceous/Tertiary Boundary', *Nature* **359**, 819–821.

Sigurdsson, H., Bonte, Ph., Turpin, L., Chaussidon, M., Metrich, N., Steinberg, M., Pradel, Ph., and D'Hondt, S.: 1991, 'Geochemical Constraints on Source Region of Cretaceous/Tertiary Impact Glasses', *Nature* **353**, 839–842.

Smit, J., Montanari, A., Swinburne, N. H. M., Alvarez, W., Hildebrand, A. R., Margolis, S. V., Claeys, P., Lowrie, W., and Asaro, F.: 1992, 'Tektite-Bearing, Deep-Water Clastic Unit at the Cretaceous-Tertiary Boundary in Northwestern Mexico', *Geology* **20**, 99–103.

Soki, R., Gaona-Vizcayno, S., Perry, E., and Villasuso-Pino, M.: 1984, 'A Chemical Drill: Sulfur Isotope Evidence for the Mechanism of Formation of Deep Sinkholes in Tropical Karst, Yucatan, Mexico', *Geological Society of America, Abstracts and Programs* **16**, 662.

Solomon, S. C. and Duxbury, E. D.: 1987, 'A Test of the Longevity of Impact-Induced Faults as Preferred Sites for Later Tectonic Activity', Proceedings of the *17*th Lunar and Planetary Science Conference, Part 2, *Journal of Geophysical Research* **92**, E759–E768.

Swisher, III, C. C., Grajales-Nishimura, J. M., Montanari, A., Margolis, S. V., Claeys, P., Alvarez, W., Renne, P., Cedillo-Pardo, E., Maurrassee, F. J.-M. R., Curtis, G. H., Smit, J., and McWilliams, M. O.: 1992, 'Coeval $^{40}Ar/^{39}Ar$ Ages of 65.0 Million Years Ago from Chicxulub Crater Melt Rock and Cretaceous-Tertiary Boundary Tektites', *Science* **257**, 954–958.

Thomas, P. G., Masson, P., and Fleitout, 1982, 'Global Volcanism and Tectonism on Mercury – Comparison with the Moon', *Earth and Planetary Science Letters* **58**, 95–103.

Vickery, A. M., Kring, D. A., and Melosh, H. J.: 1992, 'Ejecta Associated with Large Terrestrial Impacts: Implications for the Chicxulub Impact and K/T Boundary Stratigraphy', *Lunar and Planetary Science* **XXIII**, 1473–1474.

Weidie, A. E.: 1982, 'Lineaments of the Yucatan Peninsula and Fractures of the Central Quintana Roo Coast, in *Road Log and Supplement, Guidebook of the Geological Society America Meeting Field Trip No. 10*, New Orleans Geological Society, New Orleans, pp. 21–25.

Weidie, A. E.: 1985, 'Geology of Yucatan Platform', in W. C. Ward, A. E. Weidie, and W. Back (eds.), *Geology and Hydrology of the Yucatan and Quaternary Geology of Northeastern Yucatan Peninsula*, New Orleans Geological Society, New Orleans, pp. 1–19.